ACS Macro Letters

Letter

Cite This: ACS Macro Lett. 2017, 6, 1217-1222

pubs.acs.org/macroletters

Morphology Under Control: Engineering Biodegradable Stomatocytes

Imke A. B. Pijpers,[†,§] Loai K. E. A. Abdelmohsen,[†,§] David S. Williams,[*,†,‡] and Jan C. M. van Hest[*,†]

[†]Eindhoven University of Technology, P.O. Box 513 (STO 3.31), 5600MB Eindhoven, The Netherlands

[‡]Department of Chemistry, Swansea University, Swansea SA2 8PP, United Kingdom

Supporting Information

ABSTRACT: Biodegradable nanoarchitectures, with well-defined morphological features, are of great importance for nanomedical research; however, understanding (and thereby engineering) their formation is a substantial challenge. Herein, we uncover the supramolecular potential of PEG–PDLLA copolymers by exploring the physicochemical determinants that result in the transformation of spherical polymersomes into stomatocytes. To this end, we have engineered blended polymersomes (comprising copolymers with varying lengths of PEG), which undergo solvent-dependent reorganization inducing negative spontaneous membrane curvature. Under conditions of anisotropic solvent composition across the PDLLA membrane, facilitated by the dialysis methodology, we demonstrate osmotically induced stomatocyte formation as a consequence of changes in PEG solvation, inducing negative spontaneous membrane curvature. Controlled formation of unprecedented, biodegradable stomatocytes represents the unification of supramolecular engineering with the theoretical understanding of shape transformation phenomena.

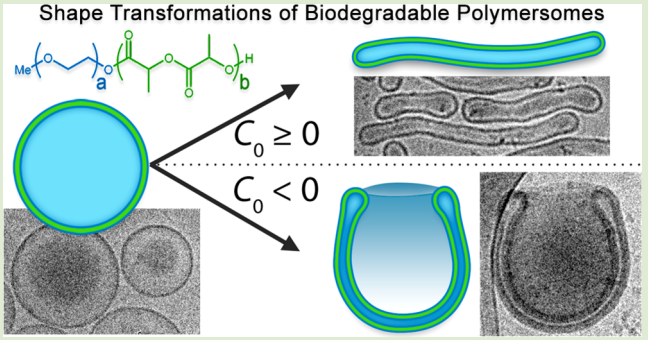

Polymeric vesicles, or polymersomes, are spherical bilayered structures formed via spontaneous self-assembly of block copolymers. During self-assembly, hydrophobic forces induce the configuration of amphiphilic copolymers into an energetically favorable state, thereby reducing the system's free energy. Polymersomes are highly versatile structures due to the ability to tune their size, shape, membrane parameters, and surface chemistry.[1−7] Moreover, the ability of polymersomes to encapsulate and compartmentalize functional materials enhances their utility toward nanomedical applications and in generating biomimetic nanosystems.[8−14] In order to enhance the functional capacity of polymersomal technologies, the ability to induce shape transformations is an exciting prospect whereby converting spherical structures into oblates (discs/stomatocytes) or prolates (tubes) can unlock new opportunities.[15,16] In particular, stomatocytes, bowl-shaped polymersomes with an opening connecting the "stomach" to the outer environment, are compelling dual-compartmentalized nanostructures capable of encapsulating enzymatic networks toward the formation of complex nanoreactors and nanomotors.[17−25]

The bulk of research in this area has up to now focused on reshaping polymersomes comprising nonbiodegradable poly(ethylene glycol)-*block*-poly(styrene) (PEG–PS)[24−26] or poly(ethylene glycol)-*block*-poly(dimethylsiloxane) (PEG–PDMS) as the main structural element,[22] which has been indispensable in developing our understanding of polymersomal shape transformations. However, the lack of full biodegradability in such systems severely limits their utility in nanomedical applications.[27] Therefore, we look to the utilization of biodegradable copolymers in order to engineer novel copolymeric architectures with tailored shapes. To this end, we have recently presented the shape transformation of biodegradable poly(ethylene glycol)-*block*-poly(D,L-lactide) (PEG- PDLLA) into prolate nanotubes utilizing a dialysis methodology.[28] However, there remains, until now, no unifying understanding of the chemical basis for this shape transformation process and how a single copolymeric system can be tuned toward both oblates and prolates. Therefore, adopting a molecular engineering approach to making biodegradable stomatocyte nanostructures, utilizing PEG–PDLLA, would close the gap between the theoretical and empirical knowledge of (osmotically induced) polymersomal shape transformations. Herein, we demonstrate the formation of PEG–PDLLA stomatocytes through engineering of the membrane composition in order to induce negative membrane curvature, thereby directing shape transformation via the oblate pathway.

The biodegradability and self-assembly properties of poly(lactide) copolymers have been reported by a number of authors.[29−31] In our previous work, describing the formation of nanotubular structures from polymersomes comprising PEG_{22}–$PDLLA_{45}$ copolymers, we highlighted the role of spontaneous curvature (C_0) as a critical factor in directing the shape

Received: September 16, 2017
Accepted: October 17, 2017
Published: October 19, 2017

DOI: 10.1021/acsmacrolett.7b00723
ACS Macro Lett. 2017, 6, 1217−1222

transformation process. Equation 1 describes the bending energy of the membrane (E_b), expressed in terms of the bending rigidity of the membrane (k), the mean surface curvature (C), and C_0:

$$E_b = \frac{k}{2}\oint(2C - C_0)^2 dA \quad (1)$$

Although the role of C_0 in the shape transformations of bilayer membranes has been extensively discussed, there are few reports that actually demonstrate the physicochemical origins of this property in the lab. Formerly, we demonstrated that rigid PEG−PS-based polymersomes can be transformed into stomatocytes by tailoring the self-assembly protocol. Our work toward understanding the thermodynamics of the PEG−PS shape transformation process informed us that, in accordance with existing theory, the role of C_0 is such that values ≥0 or values <0 would direct transformations of spherical polymersomes toward the prolate or oblate pathway, respectively (Figure 1A).[32−35] In order to expand our knowledge into shape transformations of in particular biodegradable block copolymers, we first need to fulfill these essential prerequisites: (i) copolymers should form spherical polymersomes, (ii) copolymer rigidity should be sufficient to sustain membrane curvature, and (iii) semipermeability of the membrane should facilitate osmotically induced volume reduction. Thereafter, the physicochemical origins of C_0 (and therefore the shape transformation process) can be investigated through systematic engineering of PEG−PDLLA copolymers, and their self-assembly, toward oblate stomatocyte formation (as a complement to our existing work toward formation of prolate nanotubes, Figure 1A).

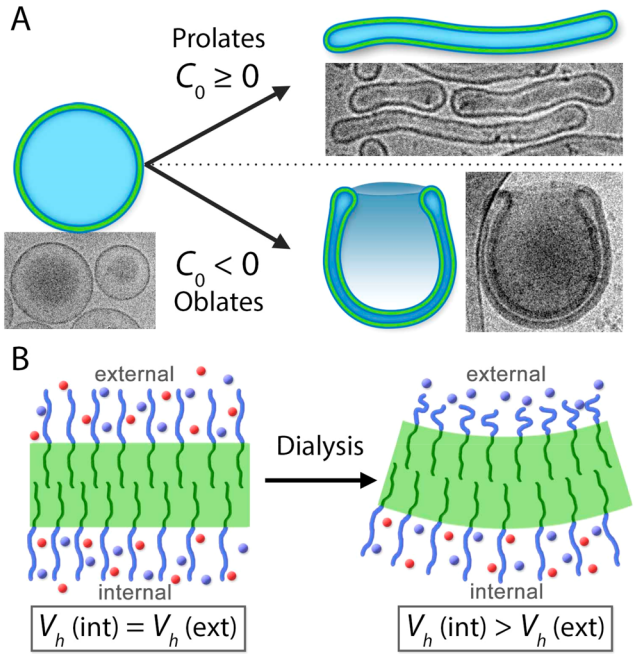

Figure 1. Schematic highlighting: (A) the influence of spontaneous curvature (C_0) upon the osmotically induced shape transformations of spherical polymersomes into prolates (tubes) or oblates (stomatocytes) and (B) the proposed mechanism for inducing negative membrane curvature toward stomatocyte formation. In our strategy, transient negative C_0 is induced in a PEG−PDLLA membrane by rapid removal of organic solvent molecules (red spheres) from the external microenvironment (by dialysis) leading to anisotropic hydrodynamic chain volume (V_h) of PEG between the exterior and interior surfaces.

Until now, systematic studies into the physical origins of C_0 have been largely performed using lipid vesicles (liposomes). Computational simulations of liposomes have demonstrated that subtle changes in headgroup interactions (either intermolecularly or with the solvent) between the inner and outer membrane surfaces can induce C_0, resulting in shape transformations.[36] Practically, it has been shown that liposomal tubulation can be induced through biomolecule binding on the external membrane surface.[33] From this work, we understand that inducing physicochemical anisotropy between the inner and outer envelopes of a vesicular membrane is the key to inducing (and controlling) C_0 and, by association, shape transformations. In contrast to lipids, copolymeric membranes possess hydrated PEG chains at their internal and external surfaces, which can be an excellent chemical handle with which to gain control over shape transformations.

In our previous work, forming nanotubes from PEG_{22}−$PDLLA_{45}$ polymersomes, we postulated that a membrane comprising 1 kDa PEG and a 15 nm thick PDLLA bilayer was not sufficient to induce substantial C_0, resulting in prolate formation (upper pathway, Figure 1A). However, through analogy with the liposomal system, we anticipate that increasing the length of surface PEG chains and increasing the PDLLA membrane thickness will allow us to explore, and control, the shape transformation process toward oblates. It is understood that PEG chain expansion, quantified by the hydrodynamic chain volume (V_h), is dependent on solvent composition, with low-dielectric organic solvents, such as THF ($\varepsilon = 7.5$), having a greater solvating power than water ($\varepsilon = 78.3$).[37] PEG solvation, and thereby the degree of expansion of the polymer chains, can be a powerful tool in conceptualizing the physicochemical origins of C_0 in this system.[38,39] We postulate that transient changes in PEG conformation arise during the dialysis process, whereby internal and external solvent compositions are disproportionately altered due to the presence of a semipermeable polymeric membrane, providing a steric driving force for the induction of C_0. Therefore, we anticipate that trans-membrane solvent anisotropy (induced during dialysis, as outlined in Figure S1) can result in a partial collapse of external PEG chains (relative to those on the interior) such that V_h(int) > V_h(ext), thus inducing negative C_0 and directing shape transformation via the oblate pathway toward stomatocytes (Figure 1B). In order to realize this strategy, it is necessary to re-engineer PEG−PDLLA polymersomes with respect to (a) increasing the length of surface PEG, in order to induce negative C_0 through anisotropic polymer solvation, and (b) increasing the thickness of the PDLLA membrane, in order to support trans-membrane solvent anisotropy during the dialysis process. However, re-engineering the molecular composition of such a copolymeric system requires a creative strategy due to the limitations encountered in the self-assembly of such amphiphilic molecules into higher-order structures, such as polymersomes.

The engineering of polymersomal shape transformation is inextricably constrained by copolymer self-assembly, which is dictated by geometric (relating to the packing parameter) and environmental factors.[40] Copolymers with the same relative compositions can result in differing morphologies, as, for example, we have previously shown that PEG_{22}−$PDLLA_{45}$ forms polymersomes in contrast to PEG_{44}−$PDLLA_{90}$ that forms micelles under the same conditions.[28] In order to create

DOI: 10.1021/acsmacrolett.7b00723
ACS Macro Lett. 2017, 6, 1217−1222

polymersomes that have longer PEG chains and thicker PDLLA membrane, besides systematically varying copolymer block composition,[41,42] copolymer blending has also proved to be an effective design strategy.[43] In contrast to blending dissimilar copolymers, which can undergo nanophase separation forming polymersomes with uniquely discontinuous surface topology,[44] homogeneous copolymer blends present the opportunity to access otherwise elusive particle morphologies.[45−47] Homogeneous mixtures of micelle- and lamellar-forming copolymers can be coassembled to form nanostructures that are trapped in a local-equilibrium (nonergodic) state because the individual components do not separate out.[46,47] Moreover, the stoichiometry of mixing between copolymeric components can be tailored in order to isolate a diverse range of colloidal morphologies.[45] We therefore decided to utilize a combination of molecular engineering and blending to construct polymersome membranes with the desired properties.

Block copolymers comprising PEG_{22} or PEG_{44} and PDLLA of 45, 70, 95, and 120 repeats were synthesized via organocatalyzed ring-opening polymerization with low PDIs (<1.2) and T_g values between 21 and 36 °C (Figure S2 and Table S1).[48] As with our previous work, we employed the solvent switch methodology for self-assembly whereby a 10 wt % copolymer solution in THF/dioxane (1:4) was diluted with water up to 50% v/v at a rate of 1 mL/h with stirring. Following self-assembly, shape transformation was induced by cold dialysis (5 °C) against aqueous solutions of varying ionic strength ([NaCl] from 0−100 mM) with concurrent (osmotically induced) volume reduction and membrane deplasticization (through removal of organic solvent), key factors in the process.[28] As a starting point for formulation we chose to use an equimolar blend of PEG_{22}−$PDLLA_x$ and PEG_{44}−$PDLLA_x$ (hereafter $P_{22/44}$−$PDLLA_x$) having the same length PDLLA block. Using the aforementioned conditions presented in our previous work with 50 mM NaCl for the dialysis step, we attempted to induce self-assembly and subsequent shape transformation. It was observed that blends of $PDLLA_{70}$ and $PDLLA_{95}$ both formed stomatosomal structures of ca. 350 and 400 nm, respectively, whereas blends of $PDLLA_{45}$ formed micelles (Figure 2A−C). Without blending, copolymers of $PDLLA_{70}$ and $PDLLA_{95}$ did not form polymersomes but tended to form aggregates (PEG_{22}−PDLLA) and micelles (PEG_{44}−PDLLA) instead (Figure S3), which aptly demonstrates the value of blending in providing access to nonergodic polymersomal morphologies. In contradistinction to this, however, although blends of $PDLLA_{120}$ were observed to form sponge-phase particles (Figure S4A), it was observed that P_{44}−$PDLLA_{120}$ formed polymersomes (Figure S4B) and, thereafter, stomatocytes (Figure 2D). Membrane thicknesses of the $P_{22/44}$−$PDLLA_{70\ and\ 95}$ and P_{44}−$PDLLA_{120}$ stomatocytes were measured to be 22, 24, and 30 nm, respectively (Figure S5). In this way we have successfully demonstrated the formation of stomatocytes with a larger PEG corona and a range of membrane thicknesses (facilitated by varying copolymer composition or blending), in accordance with our prior hypothesis. Further examination of this process was conducted using a combination of cryogenic transmission electron microscopy (cryo-TEM) and light-scattering techniques for the shape characterization of the resulting polymersomal morphologies.

For further characterization, the $P_{22/44}$−$PDLLA_{95}$ system was chosen as it represents a composition that was presented in our former work but was unable to form polymersomes without

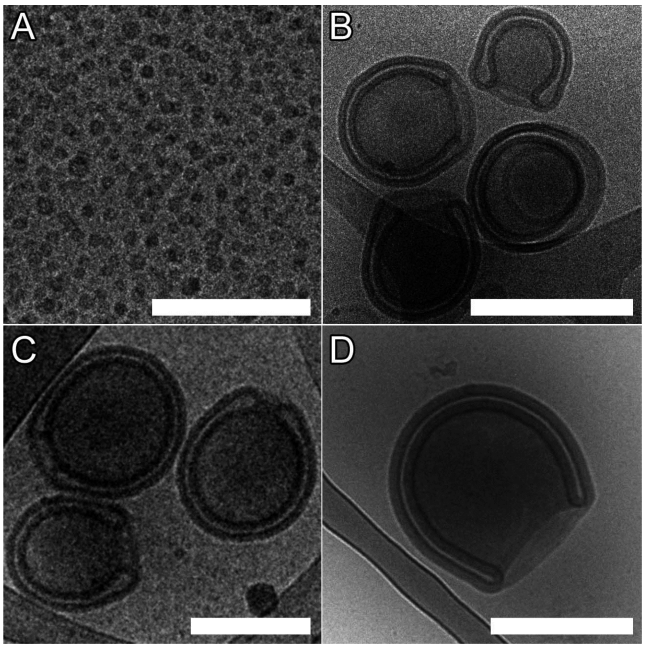

Figure 2. Cryo-TEM images of (A) $P_{22/44}$−$PDLLA_{45}$ micelles, (B) $P_{22/44}$−$PDLLA_{70}$ stomatocytes, and (C) $P_{22/44}$−$PDLLA_{95}$ and (D) P_{44}−$PDLLA_{120}$ stomatocytes (scale bars = 500 nm).

blending (Figure S6A). To further understand the shape transformation process, the effect of [NaCl] was investigated in order to explore and quantify the amount of control we could achieve in this process. Dialysis at 5 °C against pure water yielded discoidal structures, an intermediate morphology between spheres and stomatocytes,[32] formed through partial volume reduction as a consequence of out flow of organic solvent and partial deflation into insipient oblate structures (Figures 3B and S6B). Dialysis against salt solution enhanced polymersome deflation by introducing an increasing osmotic component to the outflow of internal solvent. Using 10 mM NaCl, it was evident that all structures were proceeding via the oblate pathway; however, a heterogeneous mixture of discs and open stomatocytes was formed under these conditions (Figure S6C). A population of well-structured stomatocytes was generated by dialysis against NaCl at 50 and 100 mM, with increasing volume reduction being quantified as the average neck size decreased from 127 ± 60 to 47 ± 25 nm (Figures 3C−D and S7). One consequence of the fabrication process, utilizing lab dialysis apparatus, was that in the ripened stomatocyte samples there was a subpopulation of nested polymersomes (where no neck was obvious from cryo-TEM images) that increased from ca. 15 to 25% with dialysis at 50 and 100 mM NaCl, respectively. This represents a shortcoming in the macroengineering, which necessitates more careful control over stirring and solution homogeneity, and is a consequence of the inherent sensitivity in this system. Indeed, dynamic light-scattering (DLS) data indicate that substantial deflation occurs within the first 5 min of dialysis, where the hydrodynamic diameter (D_h) decreased by ca. 40% from 693 to 454 nm (all PDI values were lower than ≤0.1), and a further 6% deflation occurring over the next 30 min, whereafter D_h = 414 nm (Figure 3E). Indeed, cryo-TEM images support the time course DLS measurements, with insipient stomatosomal structures being formed after 5 min and reaching maturity at 30 min, at which point open-necked stomatocytes are fully formed

DOI: 10.1021/acsmacrolett.7b00723
ACS Macro Lett. 2017, 6, 1217−1222

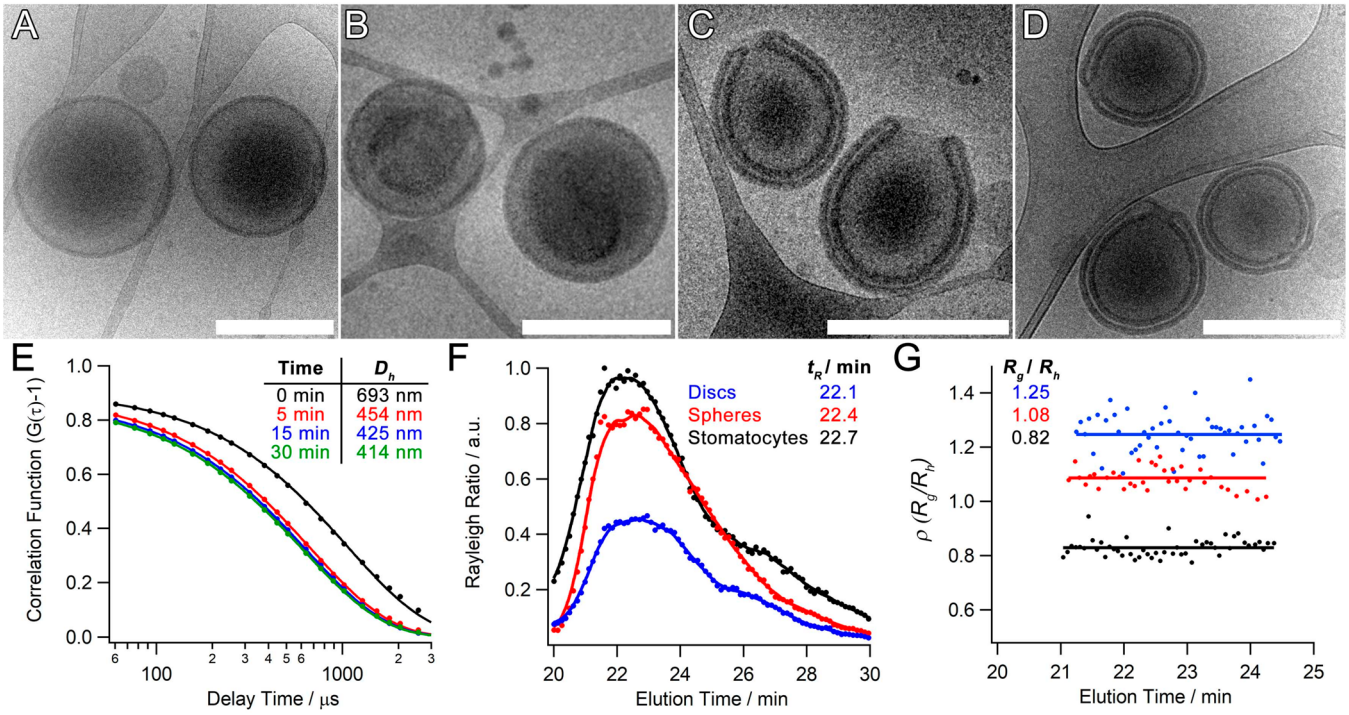

Figure 3. Cryo-TEM images of $P_{22/44}$–$PDLLA_{95}$ (A) before dialysis and after dialysis against (B) 0, (C) 50, and (D) 100 mM NaCl (scale bars = 500 nm). (E) DLS correlation data showing the reduction in hydrodynamic size during dialysis against 50 mM NaCl (cf. Cryo-TEM images in Figure S8). (F) Asymmetric flow field–flow fractionation (AF4) fractograms of $P_{22/44}$–$PDLLA_{95}$ spheres, discs, and stomatocytes alongside (G) the results of multiangle light-scattering (MALS) analysis and their respective R_g/R_h values.

(Figure S7). Quantitative assessment of this process was performed using asymmetric flow field–flow fractionation (AF4) in combination with static (SLS) and dynamic light scattering (DLS), a powerful counterpart to cryo-TEM, which can provide more insight into the shape change process (Table S2). The combination of multiangle SLS and DLS provides data on the radius of gyration (R_g) and hydrodynamic radius (R_h), respectively, for the entire particle population; the ratio of R_g/R_h, or shape ratio (ρ), provides insight into particle morphology. Elution profiles of $P_{22/44}$–$PDLLA_{95}$ polymersomes before dialysis (spheres), after dialysis in water (discs), and 50 mM NaCl (stomatocytes) were in good accordance to previous samples (Figure 3F).[18] Significantly, the values obtained were in agreement with the prior observation with discoidal, spherical, and stomatosomal polymersomes having ρ values of 1.25 ± 0.07, 1.08 ± 0.04, and 0.82 ± 0.04, respectively.[17−19] Having successfully demonstrated the formation of stomatocyte nanostructures, a final demonstration of control in this system was to induce the reverse process. Through the readdition of organic solvent, at 50 vol % (1:4 THF/dioxane), rigid stomatocytes can be reverted to spherical polymersomes by reverse dialysis (in 50 mM NaCl at 5 °C). As the organic solvent replasticizes the PDLLA membrane it facilitates inversion as the system reverts to its (energetically favorable) spherical state over the course of 1−2 h (Figures 4 and S9).

In summary, we have demonstrated the controlled formation of biodegradable stomatocytes through the osmotically induced shape transformation of PEG–PDLLA spherical polymersomes. Spherical polymersomes were constructed by rational engineering of both the molecular composition and fabrication process, giving control over the length of surface PEG and membrane thickness. In contrast to our former work on PEG–

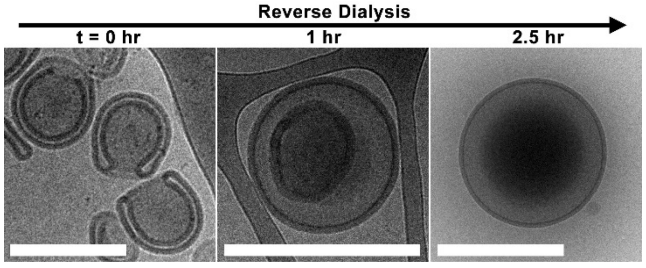

Figure 4. Cryo-TEM images tracking the reverse dialysis process as stomatocytes are reverted to spherical polymersomes after dialysis against 50 vol % organic solvent (scale bars = 500 nm).

PDLLA nanotubes, the structural characteristics of this system successfully directed the osmotically induced shape transformation down the oblate, rather than prolate, pathway. This work demonstrates that subtle changes in the chemical composition of such self-assembled architectures can have significant consequences for their physicochemical properties. Control over this shape transformation process was demonstrated by the reversibility of the system, where spherical polymersomes could be obtained by admixing organic solvent. This conceptually new approach to form stomatosomal structures from biodegradable PEG–PDLLA copolymers not only aids in deepening our fundamental understanding of shape transformations of polymersomes but also is a crucial step toward developing versatile biodegradable nanosystems, such as nanomotors and nanoreactors, in a biomedical context.

DOI: 10.1021/acsmacrolett.7b00723
ACS Macro Lett. 2017, 6, 1217−1222

■ ASSOCIATED CONTENT

Supporting Information

The Supporting Information is available free of charge on the ACS Publications website at DOI: 10.1021/acsmacrolett.7b00723.

Included are details of all materials, methods, and experimental procedures utilized in this work alongside copolymer characterization and additional cryo-TEM images of copolymer self-assembly (PDF)

■ AUTHOR INFORMATION

Corresponding Authors

*Jan C. M. van Hest (j.c.m.v.hest@tue.nl).

*David S. Williams (d.s.williams@swansea.ac.uk).

ORCID

Loai K. E. A. Abdelmohsen: 0000-0002-0094-1893

David S. Williams: 0000-0002-8209-6899

Jan C. M. van Hest: 0000-0001-7973-2404

Author Contributions

§I.A.B.P. and L.K.E.A.A. contributed equally.

Notes

The authors declare no competing financial interest.

■ ACKNOWLEDGMENTS

Authors acknowledge the support from the Ministry of Education, Culture and Science (Gravitation program 024.001.035), NWO-NSFC Advanced Materials (project 792.001.015), and the ERC Advanced grant Artisym 694120. We would also like to thank Alex Mason for help with Cryo-TEM measurements.

■ REFERENCES

(1) Zhang, X.; Tanner, P.; Graff, A.; Palivan, C. G.; Meier, W. Mimicking the cell membrane with block copolymer membranes. *J. Polym. Sci., Part A: Polym. Chem.* **2012**, *50*, 2293−2318.

(2) Peters, R. J. R. W.; Louzao, I.; van Hest, J. C. M. From polymeric nanoreactors to artificial organelles. *Chem. Sci.* **2012**, *3*, 335−342.

(3) Mai, Y.; Eisenberg, A. Self-assembly of block copolymers. *Chem. Soc. Rev.* **2012**, *41*, 5969−5985.

(4) LoPresti, C.; Lomas, H.; Massignani, M.; Smart, T.; Battaglia, G. Polymersomes: nature inspired nanometer sized compartments. *J. Mater. Chem.* **2009**, *19*, 3557−3576.

(5) Rodríguez-Hernández, J.; Chécot, F.; Gnanou, Y.; Lecommandoux, S. Toward 'smart' nano-objects by self-assembly of block copolymers in solution. *Prog. Polym. Sci.* **2005**, *30*, 691−724.

(6) Discher, D. E.; Eisenberg, A. Polymer vesicles. *Science* **2002**, *297*, 967−973.

(7) Discher, B. M.; Won, Y.-Y.; Ege, D. S.; Lee, J. C.-M.; Bates, F. S.; Discher, D. E.; Hammer, D. A. Polymersomes: Tough Vesicles Made from Diblock Copolymers. *Science* **1999**, *284*, 1143−1146.

(8) Buddingh', B. C.; van Hest, J. C. M. Artificial Cells: Synthetic Compartments with Life-like Functionality and Adaptivity. *Acc. Chem. Res.* **2017**, *50*, 769−777.

(9) York-Duran, M. J.; Godoy-Gallardo, M.; Labay, C.; Urquhart, A. J.; Andresen, T. L.; Hosta-Rigau, L. Recent advances in compartmentalized synthetic architectures as drug carriers, cell mimics and artificial organelles. *Colloids Surf., B* **2017**, *152*, 199−213.

(10) Balasubramanian, V.; Herranz-Blanco, B.; Almeida, P. V.; Hirvonen, J.; Santos, H. A. Multifaceted polymersome platforms: Spanning from self-assembly to drug delivery and protocells. *Prog. Polym. Sci.* **2016**, *60*, 51−85.

(11) Thingholm, B.; Schattling, P.; Zhang, Y.; Städler, B. Subcompartmentalized Nanoreactors as Artificial Organelle with Intracellular Activity. *Small* **2016**, *12*, 1806−1814.

(12) Gaitzsch, J.; Huang, X.; Voit, B. Engineering Functional Polymer Capsules toward Smart Nanoreactors. *Chem. Rev.* **2016**, *116*, 1053−1093.

(13) Palivan, C. G.; Goers, R.; Najer, A.; Zhang, X.; Car, A.; Meier, W. Bioinspired polymer vesicles and membranes for biological and medical applications. *Chem. Soc. Rev.* **2016**, *45*, 377−411.

(14) Blanazs, A.; Armes, S. P.; Ryan, A. J. Self-assembled block copolymer aggregates: From micelles to vesicles and their biological applications. *Macromol. Rapid Commun.* **2009**, *30*, 267−277.

(15) Yuan, H.; Huang, C.; Zhang, S. Dynamic shape transformations of fluid vesicles. *Soft Matter* **2010**, *6*, 4571−4579.

(16) Kozlovskaya, V.; Xue, B.; Kharlampieva, E. Shape-Adaptable Polymeric Particles for Controlled Delivery. *Macromolecules* **2016**, *49*, 8373−8386.

(17) Nijemeisland, M.; Abdelmohsen, L. K. E. A.; Huck, W. T. S.; Wilson, D. A.; van Hest, J. C. M. A Compartmentalized Out-of-Equilibrium Enzymatic Reaction Network for Sustained Autonomous Movement. *ACS Cent. Sci.* **2016**, *2*, 843−84.

(18) Abdelmohsen, L. K. E. A.; Rikken, R. S. M.; Christianen, P. C. M.; van Hest, J. C. M.; Wilson, D. A. Shape characterization of polymersome morphologies via light scattering techniques. *Polymer* **2016**, *107*, 445−449.

(19) Abdelmohsen, L. K. E. A.; Nijemeisland, M.; Pawar, G. M.; Janssen, G. J. A.; Nolte, R. J. M.; Van Hest, J. C. M.; Wilson, D. A. Dynamic Loading and Unloading of Proteins in Polymeric Stomatocytes: Formation of an Enzyme-Loaded Supramolecular Nanomotor. *ACS Nano* **2016**, *10*, 2652−2660.

(20) Meeuwissen, S. A.; Bruekers, S. M. C.; Chen, Y.; Pochan, D. J.; van Hest, J. C. M. Spontaneous shape changes in polymersomes via polymer/polymer segregation. *Polym. Chem.* **2014**, *5*, 489−501.

(21) Rikken, R. S. M.; Kerkenaar, H. H. M.; Nolte, R. J. M.; Maan, J. C.; van Hest, J. C. M.; Christianen, P. C. M.; Wilson, D. A. Probing morphological changes in polymersomes with magnetic birefringence. *Chem. Commun.* **2014**, *50*, 5394−5396.

(22) Salva, R.; Le Meins, J.-F.; Sandre, O.; Brûlet, A.; Schmutz, M.; Guenoun, P.; Lecommandoux, S. Polymersome Shape Transformation at the Nanoscale. *ACS Nano* **2013**, *7*, 9298−9311.

(23) Wilson, D. A.; Nolte, R. J. M.; van Hest, J. C. M. Autonomous movement of platinum-loaded stomatocytes. *Nat. Chem.* **2012**, *4*, 268−274.

(24) Meeuwissen, S. A.; Kim, K. T.; Chen, Y.; Pochan, D. J.; van Hest, J. C. M. Controlled shape transformation of polymersome stomatocytes. *Angew. Chem., Int. Ed.* **2011**, *50*, 7070−7073.

(25) Kim, K. T.; Zhu, J.; Meeuwissen, S. A.; Cornelissen, J. J. L. M.; Pochan, D. J.; Nolte, R. J. M.; van Hest, J. C. M. Controlled shape transformation of polymersome stomatocytes. *J. Am. Chem. Soc.* **2010**, *132*, 12522−12524.

(26) Lim Soo, P.; Eisenberg, A. Preparation of block copolymer vesicles in solution. *J. Polym. Sci., Part B: Polym. Phys.* **2004**, *42*, 923−938.

(27) Tu, Y.; Peng, F.; André, A. A. M.; Men, Y.; Srinivas, M.; Wilson, D. A. Biodegradable Hybrid Stomatocyte Nanomotors for Drug Delivery. *ACS Nano* **2017**, *11*, 1957−1963.

(28) Abdelmohsen, L. K. E. A.; Williams, D. S.; Pille, J.; Ozel, S. G.; Rikken, R. S. M.; Wilson, D. A.; van Hest, J. C. M. Formation of Well-Defined, Functional Nanotubes via Osmotically Induced Shape Transformation of Biodegradable Polymersomes. *J. Am. Chem. Soc.* **2016**, *138*, 9353−9356.

(29) Meng, F.; Hiemstra, C.; Engbers, G. H. M.; Feijen, J. Biodegradable polymersomes. *Macromolecules* **2003**, *36*, 3004−3006.

(30) Samarajeewa, S.; Shrestha, R.; Li, Y.; Wooley, K. L. Degradability of Poly(Lactic Acid)-Containing Nanoparticles: Enzymatic Access through a Cross-Linked Shell Barrier. *J. Am. Chem. Soc.* **2012**, *134*, 1235−1242.

(31) Fukushima, K.; Feijoo, J. L.; Yang, M.-C. Comparison of abiotic and biotic degradation of PDLLA, PCL and partially miscible PDLLA/PCL blend. *Eur. Polym. J.* **2013**, *49*, 706−717.

(32) Rikken, R. S. M.; Engelkamp, H.; Nolte, R. J. M.; Maan, J. C.; van Hest, J. C. M.; Wilson, D. A.; Christianen, P. C. M. Shaping

DOI: 10.1021/acsmacrolett.7b00723
ACS Macro Lett. 2017, 6, 1217−1222

polymersomes into predictable morphologies via out-of-equilibrium self-assembly. *Nat. Commun.* **2016**, *7*, 12606.
(33) Lipowsky, R. Spontaneous tubulation of membranes and vesicles reveals membrane tension generated by spontaneous curvature. *Faraday Discuss.* **2013**, *161*, 305−331.
(34) Jarić, M.; Seifert, U.; Wintz, W.; Wortis, M. Vesicular instabilities: The prolate-to-oblate transition and other shape instabilities of fluid bilayer membranes. *Phys. Rev. E: Stat. Phys., Plasmas, Fluids, Relat. Interdiscip. Top.* **1995**, *52*, 6623−6634.
(35) Seifert, U.; Berndl, K.; Lipowsky, R. Shape transformations of vesicles: Phase diagram for spontaneous- curvature and bilayer-coupling models. *Phys. Rev. A: At., Mol., Opt. Phys.* **1991**, *44*, 1182−1202.
(36) Markvoort, A. J.; van Santen, R. A.; Hilbers, P. A. J. Vesicle Shapes from Molecular Dynamics Simulations. *J. Phys. Chem. B* **2006**, *110*, 22780−22785.
(37) Dinç, C. Ö.; Kibarer, G.; Güner, A. Solubility profiles of poly(ethylene glycol)/solvent systems. II. Comparison of thermodynamic parameters from viscosity measurements. *J. Appl. Polym. Sci.* **2010**, *117*, 1100−1119.
(38) Vyhnalkova, R.; Müller, A. H. E.; Eisenberg, A. Control of Morphology and Corona Composition in Aggregates of Mixtures of PS-b-PAA and PS-b-P4VP Diblock Copolymers: Effects of Solvent, Water Content, and Mixture Composition. *Langmuir* **2014**, *30*, 13152−13163.
(39) Bang, J.; Jain, S.; Li, Z.; Lodge, T. P.; Pedersen, J. S.; Kesselman, E.; Talmon, Y. Sphere, Cylinder, and Vesicle Nanoaggregates in Poly(styrene-b-isoprene) Diblock Copolymer Solutions. *Macromolecules* **2006**, *39*, 1199−1208.
(40) Zehm, D.; Ratcliffe, L. P. D.; Armes, S. P. Synthesis of Diblock Copolymer Nanoparticles via RAFT Alcoholic Dispersion Polymerization: Effect of Block Copolymer Composition, Molecular Weight, Copolymer Concentration, and Solvent Type on the Final Particle Morphology. *Macromolecules* **2013**, *46*, 128−139.
(41) Löbling, T. I.; Borisov, O.; Haataja, J. S.; Ikkala, O.; Gröschel, A. H.; Müller, A. H. E. Rational design of ABC triblock terpolymer solution nanostructures with controlled patch morphology. *Nat. Commun.* **2016**, *7*, 12097.
(42) Bermudez, H.; Brannan, A. K.; Hammer, D. A.; Bates, F. S.; Discher, D. E. Molecular weight dependence of polymersome membrane structure, elasticity, and stability. *Macromolecules* **2002**, *35*, 8203−8208.
(43) Greenall, M. J.; Schuetz, P.; Furzeland, S.; Atkins, D.; Buzza, D. M. A.; Butler, M. F.; McLeish, T. C. B. Controlling the Self-Assembly of Binary Copolymer Mixtures in Solution through Molecular Architecture. *Macromolecules* **2011**, *44*, 5510−5519.
(44) LoPresti, C.; Massignani, M.; Fernyhough, C.; Blanazs, A.; Ryan, A. J.; Madsen, J.; Warren, N. J.; Armes, S. P.; Lewis, A. L.; Chirasatitsin, S.; Engler, A. J.; Battaglia, G. Controlling Polymersome Surface Topology at the Nanoscale by Membrane Confined Polymer/Polymer Phase Separation. *ACS Nano* **2011**, *5*, 1775−1784.
(45) Cho, A.; La, Y.; Jeoung, S.; Moon, H. R.; Ryu, J.-H.; Shin, T. J.; Kim, K. T. Mix-and-Match Assembly of Block Copolymer Blends in Solution. *Macromolecules* **2017**, *50*, 3234−3243.
(46) Schuetz, P.; Greenall, M. J.; Bent, J.; Furzeland, S.; Atkins, D.; Butler, M. F.; McLeish, T. C. B.; Buzza, D. M. A. Controlling the micellar morphology of binary PEO−PCL block copolymers in water−THF through controlled blending. *Soft Matter* **2011**, *7*, 749−759.
(47) Jain, S.; Bates, F. S. Consequences of Nonergodicity in Aqueous Binary PEO−PB Micellar Dispersions. *Macromolecules* **2004**, *37*, 1511−1523.
(48) Lohmeijer, B. G. G.; Pratt, R. C.; Leibfarth, F.; Logan, J. W.; Long, D. A.; Dove, A. P.; Nederberg, F.; Choi, J.; Wade, C.; Waymouth, R. M.; Hedrick, J. L. Guanidine and amidine organocatalysts for ring-opening polymerization of cyclic esters. *Macromolecules* **2006**, *39*, 8574−8583.

DOI: 10.1021/acsmacrolett.7b00723
ACS Macro Lett. 2017, 6, 1217−1222